HHS Public Access

Author manuscript

Cell Metab. Author manuscript; available in PMC 2018 August 01.

Published in final edited form as:

Cell Metab. 2017 August 01; 26(2): 353–360.e3. doi:10.1016/j.cmet.2017.07.010.

Loss of brain aerobic glycolysis in normal human aging

Manu S. Goyal[1,3,*], **Andrei G. Vlassenko**[1,3,*], **Tyler M. Blazey**[1], **Yi Su**[1], **Lars E. Couture**[1], **Tony J. Durbin**[1], **Randall J. Bateman**[2,3], **Tammie L.-S. Benzinger**[1,3], **John C. Morris**[2,3], and **Marcus E. Raichle**[1,3]

[1]Mallinckrodt Institute of Radiology, Washington University School of Medicine, St. Louis, Missouri, 63110, U.S.A

[2]Department of Neurology, Washington University School of Medicine, St. Louis, Missouri, 63110, U.S.A

[3]Alzheimer's Disease Research Center at the Washington University School of Medicine, St. Louis, Missouri, 63110, U.S.A

SUMMARY

The normal aging human brain experiences global decreases in metabolism, but whether this affects the topography of brain metabolism is unknown. Here we describe PET-based measurements of brain glucose uptake, oxygen utilization and blood flow in cognitively normal adults from 20 to 82 years of age. Age-related decreases in brain glucose uptake exceed that of oxygen use, resulting in loss of brain aerobic glycolysis (AG). Whereas the topographies of total brain glucose uptake, oxygen utilization and blood flow remain largely stable with age, brain AG topography changes significantly. Brain regions with high AG in young adults show the greatest change, as do regions with prolonged developmental transcriptional features (i.e., neoteny). The normal aging human brain thus undergoes characteristic metabolic changes, largely driven by global loss and topographic changes in brain AG.

eTOC

Prior work has shown that brain glucose metabolism falls with normal aging. Goyal *et al*. now find that this change in glucose metabolism is largely due to loss of aerobic glycolysis. Using PET imaging, they further demonstrate that the regional topography of brain aerobic glycolysis changes significantly with normal aging.

Correspondence may be addressed to Lead Contact, Dr. Manu S. Goyal at goyalm@wustl.edu.
*These authors contributed equally.

AUTHOR CONTRIBUTIONS

Conceptualization and Methodology, M.S.G., A.G.V. and M.E.R.; Formal Analysis, M.S.G., A.G.V, T.M.B., Y.S. and L.E.C; Investigation, all authors; Data Curation, M.S.G., A.G.V., L.E.C. and T.J.D.; Writing – Original Draft, M.S.G., A.G.V. and M.E.R.; Writing – Review & Editing, all authors; Supervision and Funding Acquisition, A.G.V., T.L-S.B., J.C.M and M.E.R.

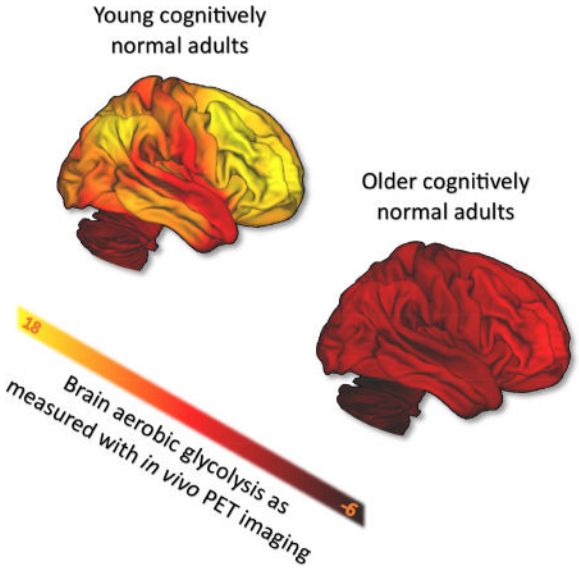

Keywords

Brain aging; brain metabolism; aerobic glycolysis; neoteny

INTRODUCTION

Normal aging is associated with changes in body appearance, physiology, and function, and likely arises from a combination of evolutionary trade-offs, environmental influences, as well as the natural degradation and failure of biological systems (Campisi, 2005; Kirkwood and Austad, 2000). The human brain also undergoes normal changes during aging, including loss in brain weight and volume (Dekaban, 1978; Fox and Schott, 2004; Scahill et al., 2003), cortical thickness (Salat et al., 2004; Sowell et al., 2003), synaptic density (Huttenlocher, 1979; Masliah et al., 1993), and a global decrement in glucose metabolism, oxygen consumption and cerebral blood flow (summarized in Goyal et al., 2014; Kety, 1956; Kuhl et al., 1982; Martin et al., 1991; Pantano et al., 1984). The reasons for these changes remain poorly understood. With regard to brain metabolism it has been tacitly assumed that changes across the normal lifespan as measured by glucose metabolism or oxygen consumption, while rarely measured together, represent a decrease in the oxidative metabolism of glucose. Our data allows us to separate the non-oxidative and oxidative fractions of glucose use in the brain, to determine whether this is true.

Human brain metabolism is unique in its high reliance on glucose utilization which accounts for 20–25% of the total body glucose consumption rate, though the brain comprises only 2% of typical human body mass (Mink et al., 1981; Raichle et al., 1970). These high metabolic rates are even higher during childhood development (summarized in Goyal et al., 2014). A characteristic feature of resting human brain glucose metabolism—particularly during development—is that it exceeds that required to account for its oxygen consumption rate by, on average, about 12–15% in young adults (Boyle et al., 1994; Dastur, 1985; Raichle et al., 1970; Vaishnavi et al., 2010) and more in children (Goyal et al., 2014). This excess glucose

utilization has been termed 'aerobic glycolysis'[1] (AG) in the human brain (Vaishnavi et al., 2010), following long-standing research on AG in cancer (Locasale and Cantley, 2011; Lunt and Vander Heiden, 2011). Several studies demonstrate that the release of lactate, a product of glycolysis, from the brain accounts for a portion of brain AG, but not its entirety (Glenn et al., 2015; Lubow et al., 2006; Madsen et al., 1999; Madsen et al., 1995; Overgaard et al., 2012; Raichle et al., 1970), leading to the hypothesis that AG is likely also related to intermediary glucose metabolism, including that associated with biosynthesis and neuroprotection via the pentose phosphate pathway (Raichle, 2015; Vlassenko and Raichle, 2015). Recent studies suggest that brain AG might be particularly relevant for synaptic plasticity and learning (Goyal et al., 2014; Magistretti, 2016; Shannon et al., 2016).

The human brain is highly neotenous (Petanjek et al., 2011; Somel et al., 2009; Somel et al., 2014). Neoteny expresses the notion that during evolution, developmental processes are prolonged and potentiated beyond that seen relative to another species; in the brain neoteny likely largely relates to prolonged periods of synaptic plasticity, myelination, and other aspects of childhood brain development. We previously identified relative differences in transcriptional neoteny among human brain regions and found that regional AG—itself a developmental metabolic feature of the brain—correlates highly with transcriptional neoteny (Goyal et al., 2014). We therefore hypothesized that the waning of neotenous processes in the brain as a part of the normal aging process, such as decreasing synaptic plasticity and completion of myelination, would lead to measurable decreases in AG as the predominant feature of metabolic change in the aging human brain.

RESULTS AND DISCUSSION

To investigate this hypothesis, we first performed a meta-analysis of previously reported whole brain measures of the cerebral metabolic rate of glucose use (CMRGlc), oxygen consumption ($CMRO_2$) and cerebral blood flow (CBF) across the adult lifespan to determine normative aging related changes in whole brain metabolism, including AG. We then applied these whole brain measurements to independent PET regional measurements of glucose use, oxygen utilization, and cerebral blood flow in 205 cognitively normal adults spanning 20 to 82 years in age.

Whole brain AG decreases with age

Whole brain measures of CMRGlc, $CMRO_2$, and CBF in cognitively normal individuals, derived largely from prior Kety-Schmidt based methods (Kety and Schmidt, 1948) or quantitative PET imaging were collected from the literature as previously described (Goyal et al., 2014) (Figure S1). These demonstrate an increase in all brain metabolism measures during childhood with a subsequent decrease during early adulthood. The decrease in CMRGlc continues during late adulthood, whereas whole brain $CMRO_2$ and CBF remain relatively unchanged as recently independently confirmed (Aanerud et al., 2016). AG

[1]To be precise, here we use the term 'aerobic glycolysis' to refer to non-oxidative metabolism of glucose— including that which leads to lactate (i.e., the Warburg Effect) as well as other intermediary pathways that do not consume oxygen. As used historically, the term 'aerobic glycolysis' refers to the fact that this occurs in the presence of oxygen, as opposed to 'anaerobic glycolysis', which occurs in the absence of oxygen.

represents the fraction of CMRGlc that is not metabolized by oxidative phosphorylation. Here we calculate AG by subtracting the fraction of CMRGlc accounted for by 6 molar equivalents of $CMRO_2$ from total CMRGlc. This is based on the 1:6 molar stoichiometric relationship between glucose and oxygen use in supplying oxidative phosphorylation. AG can be calculated at varying spatial levels: whole brain, region-wise, and at the level of individual voxels. Note that AG, as calculated in this manner, can be less than zero when substrates other than glucose, such as lactate, account for a portion of the measured $CMRO_2$.

When applying this calculation to loess fits of whole brain CMRGlc and $CMRO_2$ across adulthood (Figure S1), we find that on average AG gradually decreases with age, approximating zero at the whole brain level near the age of 60 (Figure 1). These findings are closely consistent with a prior quantitative Kety-Schmidt based study in cognitively normal active young and older adults (Dastur, 1985).

Regional changes in brain AG: Study participants and PET data

Whole brain group average assessment of aging related changes in AG obscures regional and topographic changes that might also occur with age. In order to assess aging-related changes in regional differences in brain metabolism, we collected and curated PET imaging data from 205 cognitively normal adults participating in six different studies at our institution (Figure S2). All participants underwent PET imaging to determine brain CMRGlc, $CMRO_2$, CBF, and cerebral blood volume, and MRI for image registration and partial volume correction (see Methods). Precise quantification of brain metabolism with PET typically requires invasive estimates of the arterial input function, which were not performed in this large cohort of 205 adults. As our intent here is to identify group average regional differences and inter-individual topographical changes, we instead combined literature-based whole estimates (Figure S1) with local-to-global ratios to determine quantitative regional values for each parameter of brain metabolism. Specifically, local-to-global ratios for CMRGlc, $CMRO_2$, and CBF were calculated for 78 gray and white matter brain regions and combined with the literature-based age-specific whole brain estimates to derive quantitative values for each metabolic parameter in each of the regions. These were then used to calculate regional AG as described above.

Significant outliers as determined by errors or marked deviations identified during preprocessing of the data were removed; no outliers were removed after commencing group statistical analysis. Of the remaining 205 participants, 29 underwent repeat PET imaging between 1 and 2 years later, including 19 that were amyloid imaging negative. All participants reported normal cognitive status and were verbally screened at recruitment for significant neurological or mental health illness. Nearly all participants above the age of 35 (n = 157, excluding 3 participants aged 44, 58, and 60) underwent brain amyloid imaging and were found to have either a CDR of 0 and/or normal results on Short Blessed and AD8 testing. Participants with positive amyloid imaging were excluded from further analyses to highlight normative changes in brain metabolism; thus the primary normative cohort described below includes 184 PET sessions in 165 participants.

The topography of brain metabolism changes characteristically with age

We first applied quantile normalization across the 184 individual PET sessions in the primary normative cohort with respect to each metabolic parameter (CMRGlc, $CMRO_2$, CBF, and AG) independently. For an arbitrary set of data points within any particular data sample, quantile normalization assigns the same reference quantitative values to each data point according to its rank within the sample, thereby preserving the rank order of the data points yet normalizing its statistical distribution without presuming a statistical distribution *a priori* (Bolstad et al., 2003). This method is often used in other large data domains to correct, for example, batch effects in gene expression data. In this case quantile normalization forces the region-wise data from each PET session to match one another in their quantitative histogram. Whereas this alters the absolute quantitative values for independent data points, individual differences in the topography of brain metabolism are preserved. Note that this method also effectively erases differences in the statistical distribution (e.g. mean and standard deviation) arising from differences between PET scanners or study type.

We applied principal component analysis and multidimensional scaling to the normalized data. The data is sufficiently complex that a minimum of 53 principal components are required to explain just 75% of the variance. However, the samples largely map according to participant age (Figure S3). Participant age correlates with the first principal coordinate (PC1), demonstrating that the topography, i.e. regional configuration, of brain metabolism changes significantly with age (PC1: $r = 0.56$, $p < 2\times10^{-16}$; PC2: $r = -0.11$, $p = 0.14$). The sex / gender of the participant also modestly relates to the first principal coordinate (female vs male PC1: $t = -2.75$, $p < 0.007$; PC2: $t = -0.93$, $p = 0.35$).

Aerobic glycolysis accounts for much of aging related topographic changes in brain metabolism

How do the individual forms of metabolism drive the topographic, i.e. region-wise, changes identified above? The rank order of brain regions according to a parameter of metabolism reflects the topography of that parameter of brain metabolism. To further investigate aging related changes in brain metabolism topography, we determined how Spearman rank correlations between individuals and an average baseline map from young adults (ages 20–23) vary with age. While the rank correlations remain high for CMRGlc, $CMRO_2$, and CBF throughout the adult lifespan and across individuals (CMRGlc minimum Spearman's rho = 0.92, $CMRO_2$ min rho = 0.89, CBF min rho = 0.91), AG topography changes significantly with age, becoming more and more dissimilar to young adult brain metabolism (age vs AG topography rank correlations: Pearson's $r = -0.64$, $p < 2\times10^{-16}$) (Figure 2). Multivariate analysis confirms that aging related differences in brain metabolism topography are dominated by AG topography, though the topography of other parameters change slightly also with age (multivariate general linear model: AG, $p < 2\times10^{-16}$; CBF, $p = 0.0002$; CMRGlc, $p < 0.00001$; $CMRO_2$, $p = 0.07$). These results indicate that whereas the topography of CMRGlc, $CMRO_2$, and CBF remain relativity stable during normal aging, brain AG topography varies considerably with age. This topography is not completely lost, however; the topography of brain metabolism remains somewhat similar even in the most aged participants as compared to our youngest participants.

These topographic changes mirror quantitative changes in whole brain AG. Indeed, much of the changes in brain AG topography may be due to quantitative differences in whole brain AG. Alternatively or in addition, brain AG changes might be due to aging associated changes in the topographic relationship between CMRGlc and $CMRO_2$, which theoretically can occur independent of differences in whole brain CMRGlc and $CMRO_2$. To explore these possibilities further, we calculated the Glycolytic Index (GI) across brain regions for each PET session. GI is calculated by determining the residuals after spatially regressing $CMRO_2$ from CMRGlc (Vaishnavi et al., 2010); in effect this identifies the topographic linear dissimilarity between CMRGlc and $CMRO_2$ and is thus independent of whole brain quantitative measures of metabolism. Here we find that brain GI topography also decreases significantly with age (Pearson's $r = -0.20$, $p < 0.006$), though not to the same degree as AG (Figure S4). This result suggests that changes in brain AG topography are likely due to both quantitative differences in whole brain AG as well as changes in the topographic relationship between CMRGlc and $CMRO_2$.

Neotenous brain regions show the most change in aerobic glycolysis

Till now, the analysis on the normative cohort has been limited to quantile normalized data, which represents the topography of brain metabolism. Here we now address the non-normalized data, which were derived by combining local-to-global PET imaging measurements of CMRGlc, $CMRO_2$ and CBF with whole-brain literature based estimates, and calculating AG from the regional quantitative values of CMRGlc and $CMRO_2$. We then applied loess fits to each independent region across the group. This method results in a diverse set of trajectories for AG, CMRGlc, $CMRO_2$, and CBF across all of the cortical and subcortical gray matter regions, the cerebellum, and the corpus callosum (Figure 3). Comparison of these quantitative regional AG among sex / gender matched young (21–35 year olds) and older adults (60–76 year olds) reveal several differences (Figure 4). In addition to an overall decrease in quantitative AG, there is a 'flattening' of AG across regions such that the topography of AG is readily apparent in young adults, but less so in older adults. We thus hypothesized that the degree of aging related change in a particular region would be related to its AG in young adulthood.

Across 42 cortical and subcortical gray matter regions and the cerebellum, aging related change in AG highly correlates with the degree of AG in the same regions at the start of adulthood (regional AG in young adults aged 20–23 years versus slope of change in AG: Pearson's $r = -0.87$, $p < 3\times10^{-14}$) (Figure 5a). Further, our prior work (Goyal et al., 2014) demonstrated that regions with high AG during young adulthood correlate with transcriptional neoteny, i.e., the relative persistence of gene expression that is characteristic of childhood development. The measurement of transcription neoteny in each region is restricted to the 16 regions assessed in the BrainSpan data (Kang et al., 2011) and used in our study (Goyal et al., 2014). However, among these 16 regions, the aging-related regional decrease in AG correlates also with transcriptional neoteny (regional neoteny index versus slope of change in AG: Pearson's $r = -0.79$, $p < 0.0005$) (Figure 5b). Collectively, these results suggest that aging related changes in AG predominantly occur in the most neotenous regions of the human brain.

AG loss as a biomarker of human brain aging

Our findings thus demonstrate that brain AG and its initial topography in young adults gradually wane with normal aging, particularly in the most neotenous regions of the brain. These changes occur in the absence of amyloid pathology or neurologically evident brain pathology, suggesting that they represent a 'baseline mode' of normal brain metabolism aging. The aging related loss of AG identified here might both represent underlying physiologic changes as well as harbor ill consequences to the aging brain.

Why does whole brain AG fall with age? The molecular and cellular drivers of AG in the normal human brain are not currently known. Lactate release from the brain, such as that arising from AG in the astrocyte, likely accounts for a significant portion of measured AG in the human brain (Glenn et al., 2015; Lubow et al., 2006; Madsen et al., 1999; Madsen et al., 1995; Overgaard et al., 2012; Raichle et al., 1970). The reason for net lactate release from the human brain is unclear, but rapid ATP production and volume transmission of metabolic states have been raised as putative explanations (Bergersen and Gjedde, 2012), and lactate might also have a role in potentiating the hemodynamic response locally by increasing the NADH/NAD+ ratio (Mintun et al., 2004).

However current estimates of whole brain net lactate release in young adults are not sufficient to account for the degree of whole brain AG identified here, suggesting that intermediary metabolism of glucose may also play a role in human brain metabolism (Goyal et al., 2014; Lunt and Vander Heiden, 2011). Intermediary metabolism of glucose could support neotenous processes by providing substrates directly for myelin, glycolipids and protein synthesis (Goyal et al., 2014) and/or fueling microglia in their increasingly recognized role in synaptic elimination and homeostasis (Magistretti, 2016; Shannon et al., 2016). Whereas the apportionment of brain AG to different metabolic pathways is likely complex and requires further investigation, the decrease in AG with age may in part correspond to decreases in synaptic and myelin development with age. Loss of dendritic spine turnover with age has been shown in rodents with two-photon imaging studies (Holtmaat et al., 2005; Yang et al., 2009; Zuo et al., 2005). Similarly, synaptic / spine density falls in the human brain with age, which may be associated with decreased expression of genes related to synaptic / spine development and increased expression of genes related to myelination and spine growth inhibition (Goyal and Raichle, 2013). It is currently unknown whether aging-related regional changes in cortical myelination correspond to the regional changes in brain AG identified here, but new methods and data such as that arising from the Lifespan Extension to the Human Connectome Project can directly test this hypothesis (Glasser et al., 2014).

The aging related loss of AG may also portend a loss of neuroprotection via the pentose phosphate pathway against oxidative stress, increasing the risk for oxidative damage. Many aging related conditions of the brain are associated with oxidative stress, including neurodegenerative diseases such as Parkinson Disease and Alzheimer's disease. AG related neuroprotection might normally counter the potential costs of heightened synaptic plasticity in the brain, but in the aging brain the loss of such neuroprotection could lead to heightened damage from reactive oxygen species. If true, we would predict that the neotenous regions of the human brain, i.e. regions with initially high brain AG, would be particularly

vulnerable to such forms of damage, perhaps helping to explain the link between late developing regions and their vulnerability to neurodegeneration (Douaud et al., 2014).

One limitation of our study was that it does not include measurements of brain carbohydrate consumption beyond glucose. The human brain is known to be able to use lactate and ketones for oxidative metabolism, and studies suggest that in some scenarios the human brain to some extent prefers lactate over glucose (Dienel, 2012; Smith et al., 2003). One possible explanation for some of the aging related loss of brain AG is that the aging brain may gradually switch its carbohydrate preference to lactate for oxidative metabolism. Studies of aging-related differences in brain lactate uptake would be helpful to investigate this possibility further. Changes in cerebral blood flow and vascular disease might further contribute to aging related changes in AG, and warrant further investigation. We also caution that our regional analysis of human brain AG relies on FDG-PET imaging. Though FDG has long been held as an appropriate marker of regional glucose metabolism in the human brain, exploring regional brain AG with other methods such as ^{11}C-glucose PET or ^{13}C-glucose MR spectroscopy might be helpful.

Importantly, our results demonstrate that studies of brain aging that are restricted to measuring total glucose use or cerebral blood flow are missing important aging related changes in brain metabolism including that of AG. The normative data here is provided as a supplement for future research investigations and in comparison to extant and ongoing brain aging related data. As for cancer (Liberti and Locasale, 2016), the roles and apportionment of brain AG remains unclear and requires further investigation. Comparing these data to genetic and molecular findings in humans and mechanistic findings in non-human animals may help further reveal why brain AG changes with age and reveal its consequences.

STAR METHODS

Contact for Reagent and Resource Sharing

Further information and requests for data / resources should be directed to and will be fulfilled (except for data that is restricted for access due to sensitive medical information) by the Lead Contact, Manu S. Goyal (goyalm@wustl.edu).

Experimental Model and Subject Details

Human Participants—A total of 205 individuals (59% women, self-reported sex / gender) aged 20–82 years were recruited from the Washington University community and the Knight Alzheimer Disease Research Center (ADRC). All participants had no neurological, psychiatric, or systemic medical illness that might compromise study participation. Individuals were excluded if they had contraindications to MRI, history of mental illness, possible pregnancy, or medication use that could interfere with brain function. All studies in participants coming from the Knight ADRC projects (n = 157 studies) included cognitive assessments, neurological evaluations, and clinical assessments and were cognitively normal based on the Clinical Dementia Rating (CDR) (Morris, 1993). Participants may have participated in other procedures related to the study that they were involved with, beyond those described here.

All assessments and imaging procedures were approved by Human Research Protection Office and Radioactive Drug Research Committee at Washington University in St. Louis. Written consent was provided from each participant.

Method Details

MRI—MRI scans were obtained in all individuals to guide anatomical localization. High-resolution structural images were acquired at 1.5T (Vision, Siemens, Erlangen, Germany) or 3T (Siemens TIM Trio) scanner using a 3D sagittal T1-weighted magnetization-prepared 180° radio-frequency pulses and rapid gradient-echo (MPRAGE) sequence (typical parameters: TE = 3.93ms, TR = 1900ms, TI = 1100ms, flip angle = 20°, 256 × 256 acquisition matrix, 160 slices, 1 × 1 × 1-1.3 mm voxels).

Amyloid PET imaging—All participants older than 35 years, excluding 3 (aged 44, 58, and 60, final n = 157) underwent a 60-minute dynamic Pittsburgh compound B (PIB) PET scan following injection of ~10 mCi PIB. The PIB PET imaging procedure has been described in detail (Mintun et al., 2006; Su et al., 2013), and was conducted with a Siemens model 962 ECAT EXACT HR+ PET scanner (Siemens/CTI, Knoxville, KY) or on a Siemens Biograph 40 PET/CT scanner (Siemens/CTI, Knoxville, KY). Standard uptake value ratios (SUVR) with the cerebellar cortex as reference were calculated from regions of interest with PIB-positivity defined as the mean cortical SUVR (from predefined prefrontal, parietal, and temporal regions of interest) > 1.42, a value commensurate with a mean cortical binding potential of 0.18 as defined previously for a similar cohort (Mintun et al., 2006).

CMRGlc, $CMRO_2$ and CBF PET imaging—In all but 20 individuals ^{18}F-FDG and ^{15}O PET scans were performed on a Siemens model 962 ECAT EXACT HR+ PET scanner (Siemens/CTI, Knoxville, KY) (Brix et al., 1997) and in 20 individuals, ^{18}F-FDG scans were performed on a Siemens Biograph 40 PET/CT scanner on the same or next day or (in one case) 7 weeks later to measure CMRGlc following the same protocols we have described previously (Vaishnavi et al., 2010; Vlassenko et al., 2010).

All individuals underwent one FDG scan and either one or two ^{15}O PET scans. FDG scans were performed after slow intravenous injection of 5 mCi of FDG to measure CMRGlc (Fox et al., 1988). Venous samples for plasma glucose determination were obtained just before and at the midpoint of the scan to verify that glucose levels were within normal range throughout the study. Dynamic acquisition of PET emission data continued for 60 min with twenty five 5-s frames, nine 20-s frames, ten 1-min frames, and nine 5-min frames. The last 20 min were summed to create the CMRGlc image (Fox et al., 1988; Vaishnavi et al., 2010; Vlassenko et al., 2010).

In individuals with two replicates of ^{15}O scans, CBV, CBF, and $CMRO_2$, values were averaged for data analysis. Each ^{15}O PET scan included sets of three ^{15}O scans (CO, H_2O, and O_2) to measure CBV, CBF, and $CMRO_2$ (Martin et al., 1987; Mintun et al., 1984; Raichle et al., 1983). The $CMRO_2$ parametric image was derived from the ^{15}O PET scans and corrected for CBV, using a previously described method (Vaishnavi et al., 2010; Vlassenko et al., 2010).

CBV was measured with a 5-min emission scan beginning 2 min after brief inhalation of 75 mCi of [^{15}O]CO in room air as described previously (Martin et al., 1987). Dynamic scans of 3 min with thirty five 2-s frames, six 5-s frames, and eight 10-s frames were acquired after injection of 50 mCi [^{15}O]H_2O in saline or inhalation of 60 mCi of [^{15}O]O_2 in room air, respectively for CBF and $CMRO_2$ measurements. By creating a whole-brain time-activity curve, the onset of activity in the brain could be judged exactly, allowing for a consistent selection of the optimal 40-s frame, over which activity was summed. These registrations and their corresponding transformations were performed with in-house software. Individual head movement during scanning was restricted by a thermoplastic mask. All PET images were acquired in the eyes-closed waking state. No specific instructions were given regarding cognitive activity during scanning other than to remain awake.

Quantification and Statistical Analysis

Image Analysis—The PET scans were registered to each other and then to the individual's MRI scan, which was in turn registered to an atlas representative target image, corresponding to Talairach space as defined by Lancaster et al. (Lancaster et al., 1995). The PET images were blurred and resampled into atlas space. These registrations and their corresponding transformations were performed with in-house software. Using an atlas derived brain mask, each individual's CMRGlc, CBV, CBF, and $CMRO_2$ images were scaled to have whole brain means of 1, and then same mode images, if they existed were averaged.

FreeSurfer Analysis—FreeSurfer software (Desikan et al., 2006; Fischl et al., 2002; Fischl et al., 2004) was used to segment the brain into well-defined cortical and subcortical, gray and white matter regions of interest (ROIs) based on individual MPRAGE MRI scans. These ROIs were used for regional estimation of PET parameters.

Partial volume correction—MR based partial volume correction of PET data was performed using regional spread function approach (Frouin et al., 2002), based on FreeSurfer defined ROIs (Su et al., 2015).

Quantitative calculations of regional parameters—The local-to-global images obtained as described above for CMRGlc, $CMRO_2$, and CBF were summarized to the FreeSurfer defined gray and white matter brain regions. These were then multiplied by age-specific literature-based whole brain estimates derived from loess fits for each of the metabolic parameters. Theoretically, obtaining individual Kety-Schmidt whole brain metabolism measurements alongside their PET studies might have resulted in more accurate results. However, such an invasive study would be extraordinarily expensive in over 100 participants and of questionable ethical permissibility; for example, a recent attempt to use the Kety-Schmidt method in normal adults was rejected by our Institutional Review Board on the basis that such measurements are available in the literature. Alternatively, quantitative estimates using PET have been often obtained by placing an arterial line to measure an arterial input function, which is then applied to a model to determine quantitative regional parameters; however, in addition to being invasive and likely not feasible in more than a few dozen participants, this method depends upon model assumptions that vary across studies and centers, including a lumped constant which itself is reliant on literature-based Kety-

Schmidt based measurements (Graham et al., 2002). Thus, while our method here may not be accurate at an individual level, it is likely more accurate for group-wise results as it takes advantage of data from several prior studies, and certainly more feasible in a sample size sufficiently large to identify robust aging related changes.

AG measurement—We evaluated three measures of AG: 1) oxygen/glucose index (OGI) defined by voxel-wise division of relative $CMRO_2$ by the relative CMRGlc; 2) AG defined by subtracting the oxidative fracture of CMRGlc, calculated by dividing molar $CMRO_2$ by six from total molar CMRGlc ($AG = CMRGlc - CMRO_2 \div 6$); and 3) GI defined by the residuals after spatially regressing $CMRO_2$ from CMRGlc (Vaishnavi et al., 2010). These three measures are highly correlated in our data. However OGI may be very noisy in areas of low CMRGlc as it is in the denominator, and GI does not yield interpretable quantitative values. Therefore, AG is used as the primary measure of aerobic glycolysis and has the further intuitive appeal of being larger when there is increased aerobic glycolysis, in contrast to the more historically used OGI.

Statistics—Significance was defined as $p < 0.05$. Aside from image analysis, all statistics reported in this study were calculated in R version 3.1.1.

Data and Software Availability

Raw, age-normalized, brain metabolism data in cognitively normal adults—A CSV file (AgeNormalizedBrainMetabolism.csv) is provided as Supplemental Data, which contains regional, age-normalized, partial volume corrected values for CMRGlc, $CMRO_2$, CBF, and AG for each of the 184 PET sessions in the 165 amyloid-negative individuals, as a normative data set of brain metabolism in adults.

R script and data—The R script and associated R data (which includes the data contained in the CSV file above) are provided for download from Mendeley Data (doi:10.17632/hwgvf99r7h.1) to reproduce key findings in this manuscript. The R script was used for data normalization, summary statistics and to produce several of the graphs in this manuscript.

Imaging data—The raw imaging data and/or imaging preprocessing scripts used in this study can be obtained upon request to the Lead Contact.

Additional Resources

A portion of the data came from the Dominantly Inherited Alzheimer Network (DIAN) observational trial (ClinicalTrials.gov Identifier: NCT00869817) and from the ongoing Adult Children Study; further information on these studies can be obtained at: www.dian-info.org and alzheimer.wustl.edu/Volunteer/ACS.html.

Supplementary Material

Refer to Web version on PubMed Central for supplementary material.

Acknowledgments

We are continually grateful for our participants' time and effort in this and other studies. We are also thankful for useful discussions on this work with Anish Mitra and Dr. Avi Snyder. The data presented here was the result of several independently funded efforts including grants from: The Barnes-Jewish Hospital Foundation, Charles F. and Joanne Knight, the James S. McDonnell Foundation and the McDonnell Center for Systems Neuroscience (22-3922-26239N), the Radiological Society of North America, and the National Institutes of Health (NS06833, NS057901, NS048056, MH077967, P50AG005681, P01AG003991, P01AG26276, UF1AG032438, UL1TR000448, P30NS098577, R01EB009352).

References

Aanerud J, Borghammer P, Rodell A, Jonsdottir KY, Gjedde A. Sex differences of human cortical blood flow and energy metabolism. Journal of cerebral blood flow and metabolism : official journal of the International Society of Cerebral Blood Flow and Metabolism. 2016

Bergersen LH, Gjedde A. Is lactate a volume transmitter of metabolic states of the brain? Frontiers in neuroenergetics. 2012; 4:5. [PubMed: 22457647]

Bolstad BM, Irizarry RA, Astrand M, Speed TP. A comparison of normalization methods for high density oligonucleotide array data based on variance and bias. Bioinformatics. 2003; 19:185–193. [PubMed: 12538238]

Boyle PJ, Scott JC, Krentz AJ, Nagy RJ, Comstock E, Hoffman C. Diminished brain glucose metabolism is a significant determinant for falling rates of systemic glucose utilization during sleep in normal humans. J Clin Invest. 1994; 93:529–535. [PubMed: 8113391]

Brix G, Zaers J, Adam LE, Bellemann ME, Ostertag H, Trojan H, Haberkorn U, Doll J, Oberdorfer F, Lorenz WJ. Performance evaluation of a whole-body PET scanner using the NEMA protocol. National Electrical Manufacturers Association. Journal of nuclear medicine : official publication, Society of Nuclear Medicine. 1997; 38:1614–1623.

Campisi J. Senescent cells, tumor suppression, and organismal aging: good citizens, bad neighbors. Cell. 2005; 120:513–522. [PubMed: 15734683]

Dastur DK. Cerebral blood flow and metabolism in normal human aging, pathological aging, and senile dementia. J Cereb Blood Flow Metab. 1985; 5:1–9. [PubMed: 3972914]

Dekaban AS. Changes in brain weights during the span of human life: relation of brain weights to body heights and body weights. Annals of neurology. 1978; 4:345–356. [PubMed: 727739]

Desikan RS, Segonne F, Fischl B, Quinn BT, Dickerson BC, Blacker D, Buckner RL, Dale AM, Maguire RP, Hyman BT, et al. An automated labeling system for subdividing the human cerebral cortex on MRI scans into gyral based regions of interest. Neuroimage. 2006; 31:968–980. [PubMed: 16530430]

Dienel GA. Brain lactate metabolism: the discoveries and the controversies. Journal of cerebral blood flow and metabolism : official journal of the International Society of Cerebral Blood Flow and Metabolism. 2012; 32:1107–1138.

Douaud G, Groves AR, Tamnes CK, Westlye LT, Duff EP, Engvig A, Walhovd KB, James A, Gass A, Monsch AU, et al. A common brain network links development, aging, and vulnerability to disease. Proceedings of the National Academy of Sciences of the United States of America. 2014; 111:17648–17653. [PubMed: 25422429]

Fischl B, Salat DH, Busa E, Albert M, Dieterich M, Haselgrove C, van der Kouwe A, Killiany R, Kennedy D, Klaveness S, et al. Whole brain segmentation: automated labeling of neuroanatomical structures in the human brain. Neuron. 2002; 33:341–355. [PubMed: 11832223]

Fischl B, van der Kouwe A, Destrieux C, Halgren E, Segonne F, Salat DH, Busa E, Seidman LJ, Goldstein J, Kennedy D, et al. Automatically parcellating the human cerebral cortex. Cereb Cortex. 2004; 14:11–22. [PubMed: 14654453]

Fox NC, Schott JM. Imaging cerebral atrophy: normal ageing to Alzheimer's disease. Lancet. 2004; 363:392–394. [PubMed: 15074306]

Fox PT, Raichle ME, Mintun MA, Dence C. Nonoxidative glucose consumption during focal physiologic neural activity. Science. 1988; 241:462–464. [PubMed: 3260686]

Frouin V, Comtat C, Reilhac A, Gregoire MC. Correction of partial-volume effect for PET striatal imaging: fast implementation and study of robustness. Journal of nuclear medicine : official publication, Society of Nuclear Medicine. 2002; 43:1715–1726.

Glasser MF, Goyal MS, Preuss TM, Raichle ME, Van Essen DC. Trends and properties of human cerebral cortex: correlations with cortical myelin content. Neuroimage. 2014; 93(Pt 2):165–175. [PubMed: 23567887]

Glenn TC, Martin NA, Horning MA, McArthur DL, Hovda DA, Vespa P, Brooks GA. Lactate: brain fuel in human traumatic brain injury: a comparison with normal healthy control subjects. Journal of neurotrauma. 2015; 32:820–832. [PubMed: 25594628]

Goyal MS, Hawrylycz M, Miller JA, Snyder AZ, Raichle ME. Aerobic glycolysis in the human brain is associated with development and neotenous gene expression. Cell metabolism. 2014; 19:49–57. [PubMed: 24411938]

Goyal MS, Raichle ME. Gene expression-based modeling of human cortical synaptic density. Proceedings of the National Academy of Sciences of the United States of America. 2013; 110:6571–6576. [PubMed: 23576754]

Graham MM, Muzi M, Spence AM, O'Sullivan F, Lewellen TK, Link JM, Krohn KA. The FDG lumped constant in normal human brain. Journal of nuclear medicine : official publication, Society of Nuclear Medicine. 2002; 43:1157–1166.

Holtmaat AJ, Trachtenberg JT, Wilbrecht L, Shepherd GM, Zhang X, Knott GW, Svoboda K. Transient and persistent dendritic spines in the neocortex in vivo. Neuron. 2005; 45:279–291. [PubMed: 15664179]

Huttenlocher PR. Synaptic density in human frontal cortex - developmental changes and effects of aging. Brain research. 1979; 163:195–205. [PubMed: 427544]

Kang HJ, Kawasawa YI, Cheng F, Zhu Y, Xu X, Li M, Sousa AM, Pletikos M, Meyer KA, Sedmak G, et al. Spatio-temporal transcriptome of the human brain. Nature. 2011; 478:483–489. [PubMed: 22031440]

Kety SS. Human cerebral blood flow and oxygen consumption as related to aging. Journal of chronic diseases. 1956; 3:478–486. [PubMed: 13306754]

Kety SS, Schmidt CF. The Nitrous Oxide Method for the Quantitative Determination of Cerebral Blood Flow in Man: Theory, Procedure and Normal Values. J Clin Invest. 1948; 27:476–483. [PubMed: 16695568]

Kirkwood TB, Austad SN. Why do we age? Nature. 2000; 408:233–238. [PubMed: 11089980]

Kuhl DE, Metter EJ, Riege WH, Phelps ME. Effects of human aging on patterns of local cerebral glucose utilization determined by the [18F]fluorodeoxyglucose method. Journal of cerebral blood flow and metabolism : official journal of the International Society of Cerebral Blood Flow and Metabolism. 1982; 2:163–171.

Lancaster JL, Glass TG, Lankipalli BR, Downs H, Mayberg H, Fox P. A modality-indepedent approach to spatial normalization of tomographic images of the human brain. Human Brain Mapping. 1995; 3:209–223.

Liberti MV, Locasale JW. The Warburg Effect: How Does it Benefit Cancer Cells? Trends in biochemical sciences. 2016; 41:211–218. [PubMed: 26778478]

Locasale JW, Cantley LC. Metabolic flux and the regulation of mammalian cell growth. Cell metabolism. 2011; 14:443–451. [PubMed: 21982705]

Lubow JM, Pinon IG, Avogaro A, Cobelli C, Treeson DM, Mandeville KA, Toffolo G, Boyle PJ. Brain oxygen utilization is unchanged by hypoglycemia in normal humans: lactate, alanine, and leucine uptake are not sufficient to offset energy deficit. American journal of physiology Endocrinology and metabolism. 2006; 290:E149–E153. [PubMed: 16144821]

Lunt SY, Vander Heiden MG. Aerobic glycolysis: meeting the metabolic requirements of cell proliferation. Annual review of cell and developmental biology. 2011; 27:441–464.

Madsen PL, Cruz NF, Sokoloff L, Dienel GA. Cerebral oxygen/glucose ratio is low during sensory stimulation and rises above normal during recovery: excess glucose consumption during stimulation is not accounted for by lactate efflux from or accumulation in brain tissue. Journal of cerebral blood flow and metabolism : official journal of the International Society of Cerebral Blood Flow and Metabolism. 1999; 19:393–400.

Madsen PL, Hasselbalch SG, Hagemann LP, Olsen KS, Bulow J, Holm S, Wildschiodtz G, Paulson OB, Lassen NA. Persistent resetting of the cerebral oxygen/glucose uptake ratio by brain activation: evidence obtained with the Kety-Schmidt technique. Journal of cerebral blood flow and metabolism : official journal of the International Society of Cerebral Blood Flow and Metabolism. 1995; 15:485–491.

Magistretti PJ. Imaging brain aerobic glycolysis as a marker of synaptic plasticity. Proceedings of the National Academy of Sciences of the United States of America. 2016; 113:7015–7016. [PubMed: 27317739]

Martin AJ, Friston KJ, Colebatch JG, Frackowiak RS. Decreases in regional cerebral blood flow with normal aging. Journal of cerebral blood flow and metabolism : official journal of the International Society of Cerebral Blood Flow and Metabolism. 1991; 11:684–689.

Martin WR, Powers WJ, Raichle ME. Cerebral blood volume measured with inhaled C15O and positron emission tomography. J Cereb Blood Flow Metab. 1987; 7:421–426. [PubMed: 3497162]

Masliah E, Mallory M, Hansen L, DeTeresa R, Terry RD. Quantitative synaptic alterations in the human neocortex during normal aging. Neurology. 1993; 43:192–197. [PubMed: 8423884]

Mink JW, Blumenschine RJ, Adams DB. Ratio of central nervous system to body metabolism in vertebrates: its constancy and functional basis. The American journal of physiology. 1981; 241:R203–212. [PubMed: 7282965]

Mintun MA, Larossa GN, Sheline YI, Dence CS, Lee SY, Mach RH, Klunk WE, Mathis CA, DeKosky ST, Morris JC. [11C]PIB in a nondemented population: potential antecedent marker of Alzheimer disease. Neurology. 2006; 67:446–452. [PubMed: 16894106]

Mintun MA, Raichle ME, Martin WR, Herscovitch P. Brain oxygen utilization measured with O-15 radiotracers and positron emission tomography. Journal of nuclear medicine : official publication, Society of Nuclear Medicine. 1984; 25:177–187.

Mintun MA, Vlassenko AG, Rundle MM, Raichle ME. Increased lactate/pyruvate ratio augments blood flow in physiologically activated human brain. Proceedings of the National Academy of Sciences of the United States of America. 2004; 101:659–664. [PubMed: 14704276]

Morris JC. The Clinical Dementia Rating (CDR): current version and scoring rules. Neurology. 1993; 43:2412–2414.

Overgaard M, Rasmussen P, Bohm AM, Seifert T, Brassard P, Zaar M, Homann P, Evans KA, Nielsen HB, Secher NH. Hypoxia and exercise provoke both lactate release and lactate oxidation by the human brain. FASEB journal : official publication of the Federation of American Societies for Experimental Biology. 2012; 26:3012–3020. [PubMed: 22441982]

Pantano P, Baron JC, Lebrun-Grandie P, Duquesnoy N, Bousser MG, Comar D. Regional cerebral blood flow and oxygen consumption in human aging. Stroke; a journal of cerebral circulation. 1984; 15:635–641.

Petanjek Z, Judas M, Simic G, Rasin MR, Uylings HB, Rakic P, Kostovic I. Extraordinary neoteny of synaptic spines in the human prefrontal cortex. Proceedings of the National Academy of Sciences of the United States of America. 2011; 108:13281–13286. [PubMed: 21788513]

Raichle ME. The restless brain: how intrinsic activity organizes brain function. Philosophical transactions of the Royal Society of London Series B, Biological sciences. 2015:370.

Raichle ME, Martin WR, Herscovitch P, Mintun MA, Markham J. Brain blood flow measured with intravenous H2(15)O. II. Implementation and validation. Journal of nuclear medicine : official publication, Society of Nuclear Medicine. 1983; 24:790–798.

Raichle ME, Posner JB, Plum F. Cerebral blood flow during and after hyperventilation. Archives of neurology. 1970; 23:394–403. [PubMed: 5471647]

Salat DH, Buckner RL, Snyder AZ, Greve DN, Desikan RS, Busa E, Morris JC, Dale AM, Fischl B. Thinning of the cerebral cortex in aging. Cereb Cortex. 2004; 14:721–730. [PubMed: 15054051]

Scahill RI, Frost C, Jenkins R, Whitwell JL, Rossor MN, Fox NC. A longitudinal study of brain volume changes in normal aging using serial registered magnetic resonance imaging. Archives of neurology. 2003; 60:989–994. [PubMed: 12873856]

Shannon BJ, Vaishnavi SN, Vlassenko AG, Shimony JS, Rutlin J, Raichle ME. Brain aerobic glycolysis and motor adaptation learning. Proceedings of the National Academy of Sciences of the United States of America. 2016; 113:E3782–3791. [PubMed: 27217563]

Smith D, Pernet A, Hallett WA, Bingham E, Marsden PK, Amiel SA. Lactate: a preferred fuel for human brain metabolism in vivo. J Cereb Blood Flow Metab. 2003; 23:658–664. [PubMed: 12796713]

Somel M, Franz H, Yan Z, Lorenc A, Guo S, Giger T, Kelso J, Nickel B, Dannemann M, Bahn S, et al. Transcriptional neoteny in the human brain. Proceedings of the National Academy of Sciences of the United States of America. 2009; 106:5743–5748. [PubMed: 19307592]

Somel M, Rohlfs R, Liu X. Transcriptomic insights into human brain evolution: acceleration, neutrality, heterochrony. Current opinion in genetics & development. 2014; 29:110–119. [PubMed: 25233113]

Sowell ER, Peterson BS, Thompson PM, Welcome SE, Henkenius AL, Toga AW. Mapping cortical change across the human life span. Nature neuroscience. 2003; 6:309–315. [PubMed: 12548289]

Su Y, Blazey TM, Snyder AZ, Raichle ME, Marcus DS, Ances BM, Bateman RJ, Cairns NJ, Aldea P, Cash L, et al. Partial volume correction in quantitative amyloid imaging. NeuroImage. 2015; 107:55–64. [PubMed: 25485714]

Su Y, D'Angelo GM, Vlassenko AG, Zhou G, Snyder AZ, Marcus DS, Blazey TM, Christensen JJ, Vora S, Morris JC, et al. Quantitative analysis of PiB-PET with FreeSurfer ROIs. Plos One. 2013; 8:e73377. [PubMed: 24223109]

Vaishnavi SN, Vlassenko AG, Rundle MM, Snyder AZ, Mintun MA, Raichle ME. Regional aerobic glycolysis in the human brain. Proceedings of the National Academy of Sciences of the United States of America. 2010; 107:17757–17762. [PubMed: 20837536]

Vlassenko AG, Raichle ME. Brain aerobic glycolysis functions and Alzheimer's disease. Clin Transl Imaging. 2015; 3:27–37. [PubMed: 26855936]

Vlassenko AG, Vaishnavi SN, Couture L, Sacco D, Shannon BJ, Mach RH, Morris JC, Raichle ME, Mintun MA. Spatial correlation between brain aerobic glycolysis and amyloid-beta (Abeta) deposition. Proceedings of the National Academy of Sciences of the United States of America. 2010; 107:17763–17767. [PubMed: 20837517]

Yang G, Pan F, Gan WB. Stably maintained dendritic spines are associated with lifelong memories. Nature. 2009; 462:920–924. [PubMed: 19946265]

Zuo Y, Lin A, Chang P, Gan WB. Development of long-term dendritic spine stability in diverse regions of cerebral cortex. Neuron. 2005; 46:181–189. [PubMed: 15848798]

Highlights

- Whole brain aerobic glycolysis (AG) falls with normal aging in humans
- The regional topography of brain AG changes significantly with normal aging
- Neotenous regions of the brain show the largest aging-related change in AG

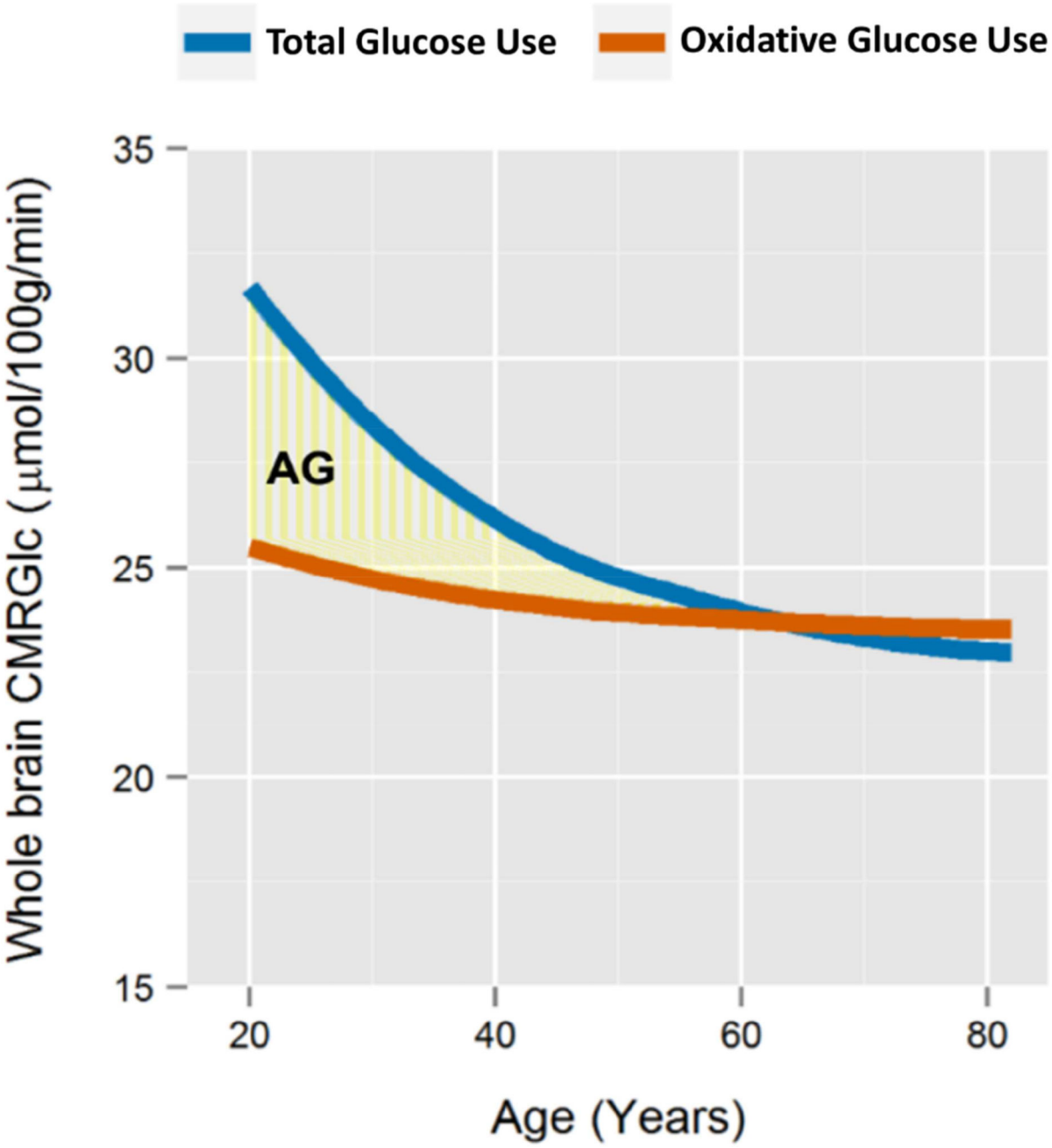

Figure 1. Meta-analysis of human whole brain metabolism

We performed and fit loess curves to a meta-analysis of prior measurements of whole brain CMRGlc ("total glucose use", blue) and $CMRO_2$ converted to glucose use equivalents based on the stoichiometric oxygen-to-glucose ratio of 6 ("oxidative glucose use", orange) (see Figure S1 for details). This shows that CMRGlc decreases significantly with age, but $CMRO_2$ does not change or only minimally so, resulting in gradual decrease in apparent whole brain AG (yellow shaded region). Apparent whole brain AG approximates zero near the age of 60. Notably, similar changes in whole brain AG between young (mean 21 years old) and older (mean 71 years old) individuals were noted by Darab Dastur in 1985 based on

multiple Kety-Schmidt measurements (Dastur, 1985), when restricting the older cohort to "physically and mentally active" healthy participants.

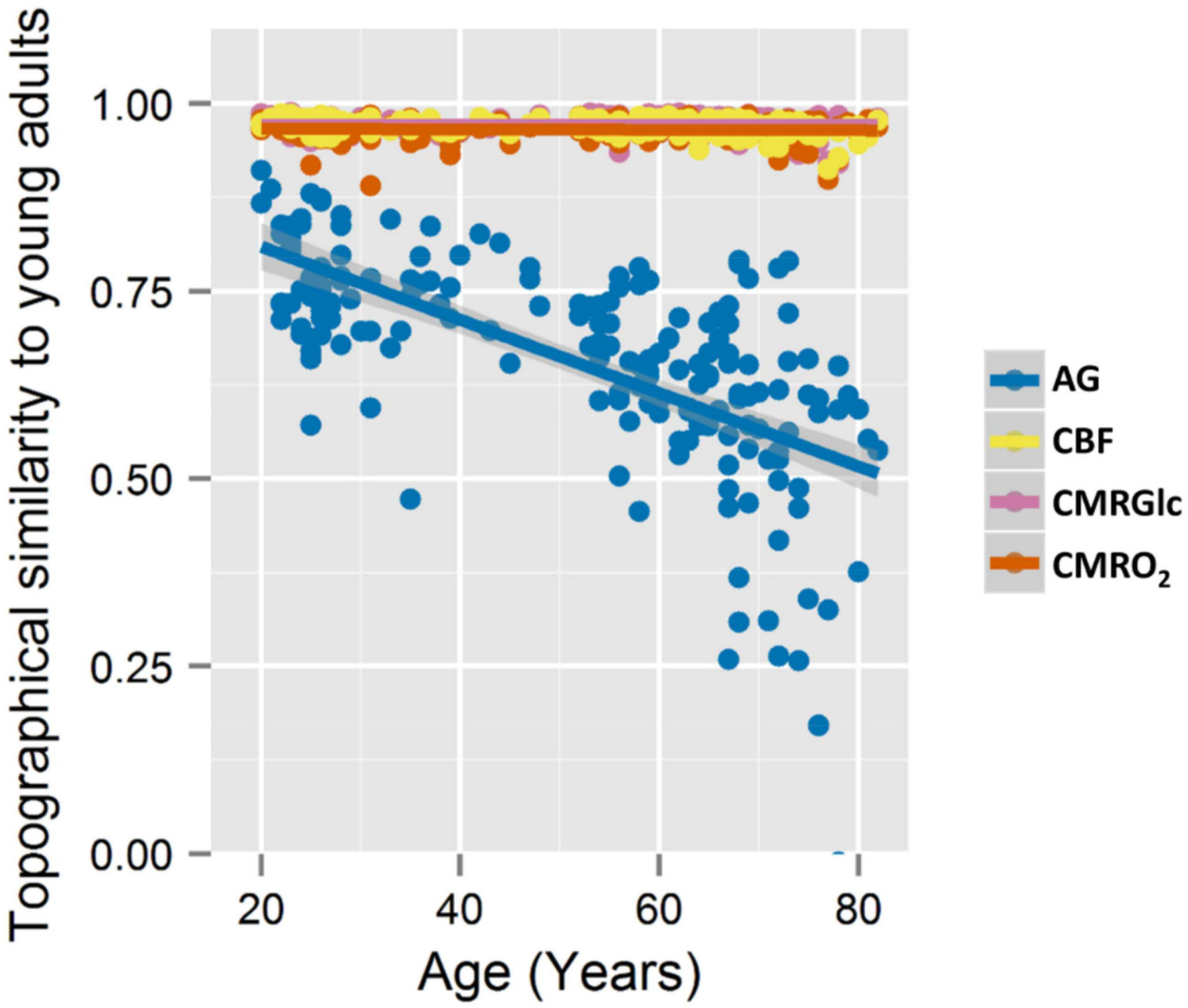

Figure 2. Brain AG topography changes with normal human aging

The normalized data for each metabolic parameter and each individual was Spearman rank correlated with an average data set comprising participants aged 20 – 23 years. For CBF (yellow), CMRGlc (pink), and $CMRO_2$ (orange), the Spearman rank correlation remained high throughout the lifespan (CMRGlc minimum Spearman's rho = 0.92, $CMRO_2$ min rho = 0.89, CBF min rho = 0.91), suggesting that the topography for these aspects of brain metabolism remains relatively stable throughout the adult lifespan. The Spearman rank correlations for AG (blue) for each participant instead shows significant decreases with age (Pearson's $r = -0.64$, $p < 2\times10^{-16}$), remaining only modestly similar to the young adults among the oldest participants. High inter-individual variability is evident for AG, particularly among the older participants. These changes in AG topography are in part due to whole brain changes in AG and in part due to topographical changes between CMRGlc and $CMRO_2$ (see Figure S4 for details).

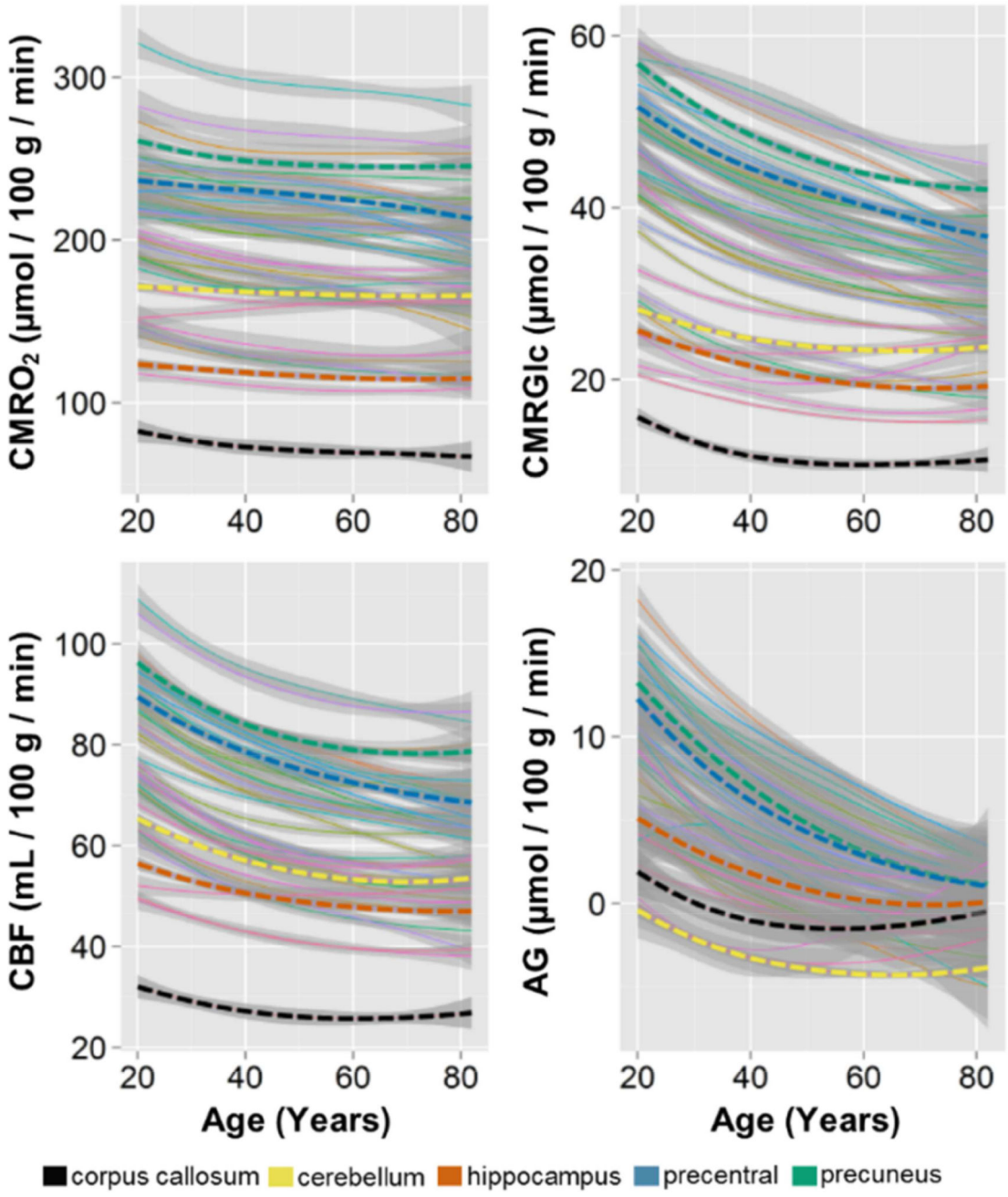

Figure 3. Summary of regional quantitative metabolic change in the human brain with aging

Literature-based whole brain estimates for $CMRO_2$, CMRGlc, CBF, and AG were combined with local-to-global ratios to determine a quantitative value in every individual in the normative cohort, for each metabolic parameter in 42 gray matter regions and the corpus callosum as a representative white matter region. These were then fit with loess curves to demonstrate the trajectory for each metabolic parameter in each of these regions. The thin lines represent each of the regions with superimposed thick dotted lines representing representative regions, as shown in the bottom legend. The shaded gray regions show the standard error about the loess curves, though it should be noted that using literature-based

whole brain estimates will necessarily obscure quantitative inter-individual variability. It is evident that with rare exception, all regions decrease in all aspects of metabolism. However, the loss of $CMRO_2$ is slight as compared to the more dramatic decrease in AG, which regionally varies in rate of change with aging. This whole-brain normalized regionally quantitative data is provided as a normative data set in the Supplemental Table.

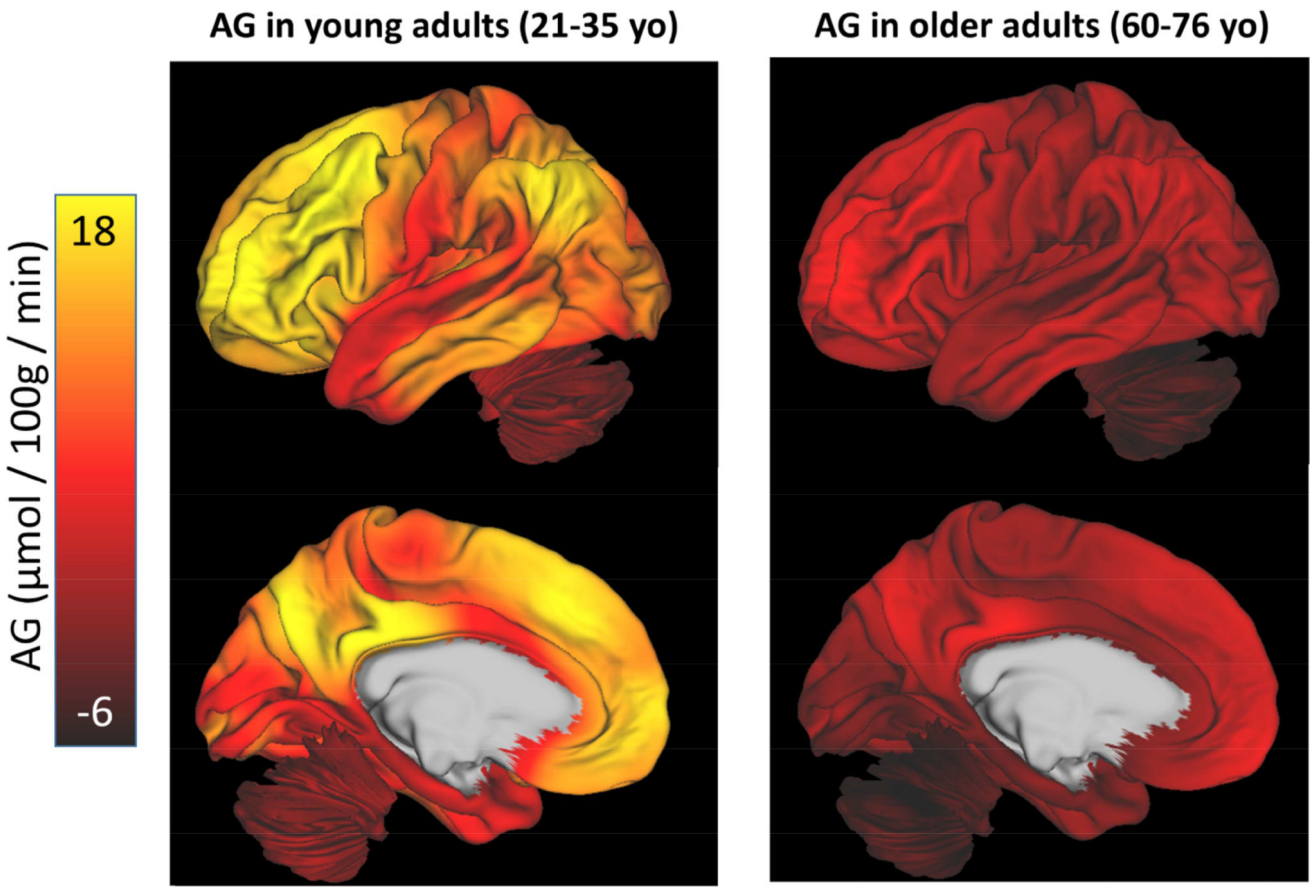

Figure 4. The topography of AG flattens with aging

Quantitative values for AG were determined by combining literature-based whole brain values for CMRGlc and $CMRO_2$ with local-to-global values within each individual (see Methods). This demonstrates that in a young cohort of adults (21–35 yo) AG varies considerably throughout the brain as has been described previously (Vaishnavi et al. 2010). In an older cohort (60–76 yo) matched for sex / gender, the overall topography of AG is flattened and depressed. Slight regional variation of AG persists in a manner similar to that seen in young adults, accounting for the modestly positive Spearman rank correlations for older adults (Figure 2). As our measurement of AG does not include other carbohydrate use for oxidative phosphorylation—such as lactate—some values of AG extend below zero, in particular in the cerebellum in the older cohort.

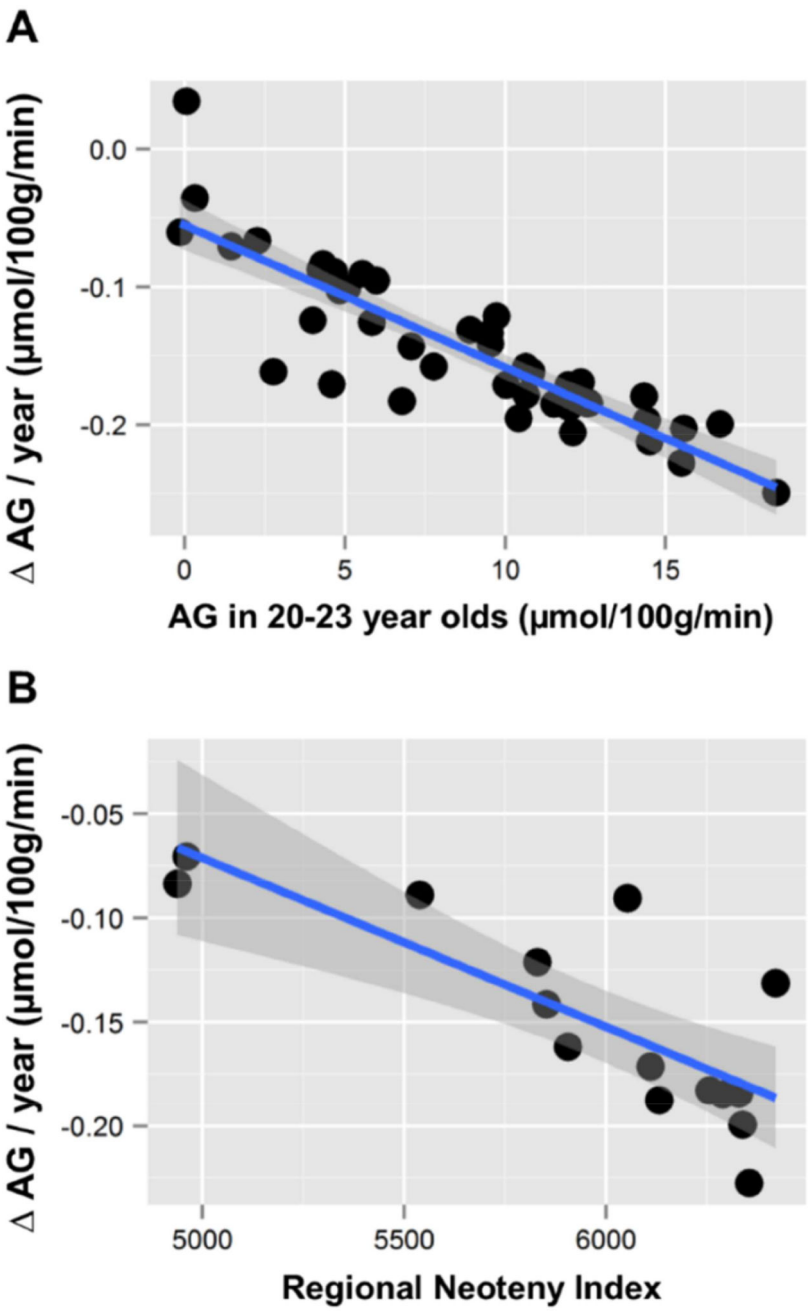

Figure 5. Regional rate of decreased AG correlates with regional metabolic and transcriptional neoteny

(A) AG was calculated for each region using the combined literature-based whole brain and local-to-global values (see Methods). Change in AG per year was then calculated for each region and compared to the AG in that region in young adults aged 20 – 23 years. Regions with the highest AG in young adults showed the most rapid loss of AG per year (Pearson's $r = -0.87$, $p < 3\times10^{-14}$), including such regions as the medial frontal cortex and the precuneus. (B) The BrainSpan lifespan human brain transcriptional data was used to calculate a regional neoteny index, which is a measure of the persistence of developmentally related gene expression (Goyal et al., 2014), for each of the 15 regions assessed by the

BrainSpan data set as compared to the cerebellum. In addition to the cerebellum, the 15 regions include dorsolateral prefrontal cortex; ventrolateral, medial and orbital frontal cortex; primary motor, somatosensory, auditory and visual cortex; posterior inferior parietal cortex; posterior superior and inferior temporal cortex; hippocampus and amygdala; striatum; and thalamus (Kang et al., 2011). The loss of AG per year for these 15 regions inversely correlates with their regional neoteny index (Pearson's $r = -0.79$, 95% CI −0.47 to −0.93, $p < 0.0005$). These results suggest that the largest aging-related change in AG occurs in the most metabolic and transcriptionally neotenous regions of the human brain, accounting for the flattening of AG seen in Figure 4.